



ELSEVIER

Available online at www.sciencedirect.com

SCIENCE @ DIRECT®

Nuclear Instruments and Methods in Physics Research A 521 (2004) 318–325

NUCLEAR
INSTRUMENTS
& METHODS
IN PHYSICS
RESEARCH
Section A

www.elsevier.com/locate/nima

Malmberg–Penning and Minimum-B trap compatibility: the advantages of higher-order multipole traps[☆]

J. Fajans*, A. Schmidt

Department of Physics, University of California, 366 LeConte Hall, Berkeley, CA 94720, USA

Received 16 June 2003; received in revised form 21 October 2003; accepted 7 November 2003

Abstract

The ATHENA and ATRAP collaborations have recently created large numbers of untrapped anti-hydrogen atoms. The most commonly suggested scheme for trapping the anti-hydrogen is to use a Minimum-B trap. Unfortunately, the Minimum-B fields are very likely to destroy the confinement of the anti-hydrogen constituents, the positrons and anti-protons, which are themselves held in double-well Malmberg–Penning traps. The reasons for the loss of confinement, and modifications to the Minimum-B trap that may alleviate this problem, are discussed in this paper.

© 2003 Elsevier B.V. All rights reserved.

PACS: 36.10. – k; 52.27.Jt; 52.55.Jd

Keywords: Non-neutral plasma; Anti-hydrogen; Minimum-B trap; Malmberg–Penning trap; Transport; ATHENA; ATRAP

1. Introduction

Two recent experiments at CERN have had remarkable success generating anti-hydrogen ($\bar{\text{H}}$) [1–3]¹. The two experiments differ in details, but both experiments employ double-well, Malmberg–Penning traps (see Fig. 1) to hold and cool the anti-hydrogen constituents: positrons (e^+), and anti-protons (\bar{p}). Malmberg–Penning traps use strong axial magnetic fields to keep particles from

escaping radially, and electrostatic wells to keep them from escaping axially. “Double-well” Malmberg–Penning traps confine oppositely charged particles by using adjacent wells of different sign. In the experiments considered here, temperature effects or “sloshing” are used to make the anti-hydrogen constituents overlap, and, occasionally, form anti-hydrogen through radiative or three-body recombination. Being neutral, the anti-hydrogen is not confined in the Malmberg–Penning trap. Consequently, the anti-hydrogen lasts only until it is carried into the trap wall by its initial momentum.

Ultimately, the experimenters hope to test CPT invariance by doing precision spectroscopy on anti-hydrogen; such detailed measurements can only be done on trapped anti-hydrogen. Currently, no lasers are available that can

[☆]This work was supported by the Office of Naval Research and by the National Science Foundation.

*Corresponding author. Tel.: +1-510-642-3872; fax: +1-510-643-8497.

E-mail address: joel@physics.berkeley.edu (J. Fajans).

URL: [Http://socrates.berkeley.edu/~fajans](http://socrates.berkeley.edu/~fajans).

¹More precisely, ATHENA and ATRAP are likely creating highly excited $\vec{E} \times \vec{B}$ guiding center atoms, see Ref. [3].

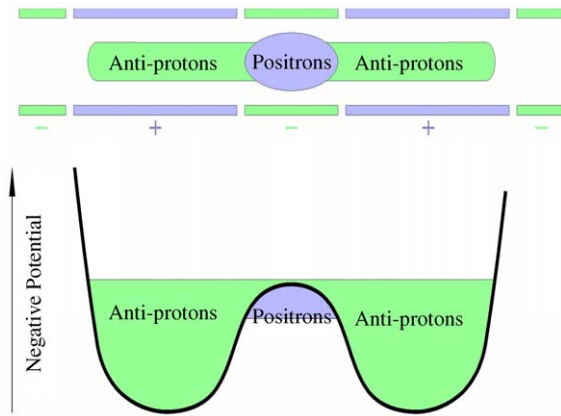


Fig. 1. Schematic diagram showing a double-well Malmberg–Penning trap similar to those used by ATHENA and ATRAP.

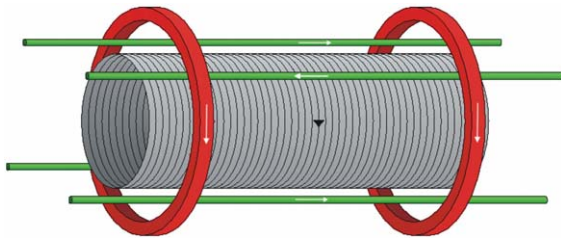


Fig. 2. The field coils for a quadrupole Minimum-B/Malmberg–Penning trap. (The electrostatic structures shown in Fig. 1 are placed inside the solenoid.) The solenoid produces the axial field for the Penning–Malmberg trap, the two end coils generate the mirror field that confines \bar{H} axially, and the four quadrupole wires generate the field that confines \bar{H} radially. This configuration is similar to a Joffe configuration. To trap \bar{H} , the mirror coils must be positioned so that the minimum in the field extends over the overlap region in Fig. 1. Because the coils induce transport, they may need to be pushed far enough away that their field is small over the entire plasma region.

efficiently trap anti-hydrogen; instead, researchers have spoken of using Minimum-B traps. Such traps use the neutral’s magnetic moment to attract the atoms to a minimum in the magnetic field.

Because the anti-hydrogen is generated inside the Malmberg–Penning trap, the Minimum-B fields must be superimposed on the Malmberg–Penning fields. Unfortunately, simple Minimum-B fields (see Fig. 2) are likely to destroy the confinement of the anti-hydrogen constituents, e^+

and \bar{p} , in the Malmberg–Penning traps; anti-hydrogen may not have enough time to be formed before the positrons and anti-protons are lost. However, using high-order multipole fields may minimize the deleterious effects of the Minimum-B fields on the constituent confinement.

2. ATHENA and ATRAP parameters

The parameters of the ATHENA and ATRAP experiments are shown in Table 1. For the discussion here, it is important to know whether the \bar{H} constituents behave like a gas of non-interacting single particles, or behave collectively, like a plasma. This distinction determines whether the orbits are determined solely by the vacuum fields imposed by the trap itself, or from the far more complicated self-consistent fields: the sum of the vacuum fields and the fields from the charged constituents themselves. It also suggests, but does not entirely determine, whether or not collisions are important. The distinction is made by comparing the constituent column dimensions to the constituent Debye lengths. (The Debye length is $\lambda_D = \sqrt{kT/4\pi n e^2}$, where T is the temperature, n is the density, and e is the unit charge.) For both ATHENA and ATRAP, the positron Debye length is much less than the positron column radius or length; the positrons are in the collective, or plasma regime. The anti-proton Debye lengths are only somewhat smaller (factors of two–seven) than the anti-proton column lengths and radii. Thus, the anti-protons are also in the plasma

Table 1
Approximate ATHENA and ATRAP System Parameters [21,22]

	ATHENA	ATRAP
Temperature	15 K	4.2 K
Solenoidal field	3 T	5.4 T
Positron density	$2 \times 10^8 \text{ cm}^{-3}$	$1 \times 10^8 \text{ cm}^{-3}$
Positron column length	3.2 cm	0.8 cm
Positron Debye length	0.0019 cm	0.0014 cm
Anti-proton density	10^4 cm^{-3}	10^4 cm^{-3}
Anti-proton column length	1.0 cm	1.0 cm
Anti-proton Debye length	0.27 cm	0.14 cm

regime, but less robustly than the positrons. Note that both the positrons and the anti-protons are far from the Brillouin limit, and diamagnetic effects are unimportant.

3. Effect of the mirror field

Axial \bar{H} confinement in Minimum-B traps is provided by a “mirror” field that peaks the field at the trap ends. Such fields can be generated by two end coils, as shown in Fig. 2. Both the e^+ and \bar{p} equilibria and transport will be affected by the mirror fields. Equilibria in mirror fields have been studied experimentally [4] and theoretically [5]. The relevant effects of the mirror field are

- (1) The e^+ and \bar{p} densities will be proportional to the magnetic field. (This is true only because the e^+ and \bar{p} form charged plasmas. If the constituents behaved like a gas of non-interacting particles the density would be independent of the field strength.)
- (2) The radii of the columns of e^+ and \bar{p} will neck down in the high field region slightly more than one would expect from following the magnetic field lines.
- (3) Charged particles with a high ratio of perpendicular to parallel energy will reflect from the increasing field; thus, particles will be trapped in the low magnetic field region.
- (4) The electric potential will *not* be constant along field lines; particles will be attracted into the high field region. Consequently:
 - The separatrix between the trapped and untrapped particles in the low field region will be significantly modified from the standard result by the potential variation.
 - Particles will also be trapped in the *high* magnetic field region. (This would not occur if the constituents behaved like a gas of non-interacting particles.)

Thus, the equilibria are substantially more complicated than those in a simple solenoidal field. The equilibria may not be as advantageous. For example, the constituent densities will be highest at the ends of the trap, underneath the

mirror coils, not in the center, where the \bar{H} generation takes place.

A more serious consequence of the mirror field is increased transport. Kabantsev and Driscoll [6] have shown that transport increases dramatically with axial magnetic field variations. The transport is thought to be due to “Trapped Particle Scattering [7]” scattering across trapped/untrapped particle separatrices. Kabantsev and Driscoll measured a five-fold increase in the transport for a 0.1% field variation. Recently [8], they report that the transport may not increase much with further increases in field variations; if so the 100% variations necessary for a satisfactory Minimum-B trap may be tolerable.

Moving the mirror field coils out beyond the extent of the Malmberg–Penning trap would prevent this transport. This solution is not ideal as the volume into which the \bar{H} is trapped would increase.

4. Effect of the multipole field

Radial neutral-particle confinement requires a magnetic field that increases with radius. Such fields can be generated by quadrupole or higher-order magnetic multipoles. The equilibria and transport in multipole fields are quite complicated.

Though the multipole field is itself axially invariant, as is the Malmberg–Penning trap’s solenoidal field, the sum of the two fields is not. For instance, the sum of a quadrupole and solenoid field produce field lines that approach the central axis at two opposing angles, and diverge from the axis at 90° from these angles (see Fig. 3).

How the constituent plasmas deform in such fields is determined by the ratio of their rotation frequency f_R , to their bounce frequency f_B . The plasmas rotate because of $\vec{E} \times \vec{B}$ drifts in its self-electric field (often called the $\vec{E} \times \vec{B}$ rotation) and the drifts in the confinement fields at the plasmas’ ends (often called the magnetron rotation). If this rotation frequency is slow compared the frequency at which the plasma particles bounce from end to end, then the plasmas will follow the field lines. For a quadrupole, the plasmas will form into a

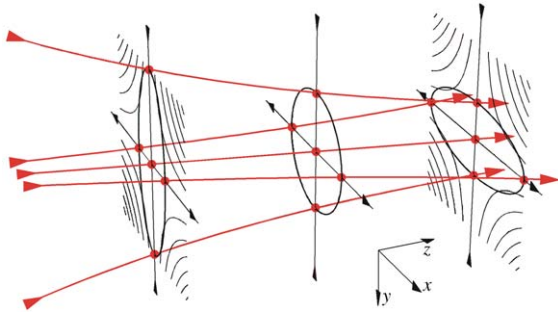


Fig. 3. Net field lines in the presence of a quadrupole and a solenoid.

Table 2
Number of rotations per transit ($f_R/2f_B$) without and with the magnetron rotation

	ATHENA	ATRAP
Self-rotation only		
Positrons	0.2	0.027
Anti-protons	0.00014	0.00014
Total rotation		
Positrons	0.2	0.028
Anti-protons	0.09	0.08

The quadrupolar resonance occurs when this ratio equals 0.25. Note that too little information is given in the literature to calculate the magnetron effects, and, thus, the total rotation frequencies, accurately.

shape similar to a twisted bow tie: circular in the center, and elliptical at the two ends, with the major radii of the ends rotated by 90° [9]. If the plasmas are rotating quickly compared to the bounce frequency, however, the rotation will average over the multipole fields and the plasmas' shape will revert to the cylinders found in the absence of the multipole. The differing shapes in the two regimes have been confirmed experimentally [9].

For the parameters given in Table 1, the rotation to bounce ratios are given in Table 2. For a quadrupole field, the plasmas are in the slowly rotating regime. Consequently they form twisted bow ties, not cylinders. For the ATHENA positrons, the bow tie shape is problematic; assuming a quadrupole field at 1 cm comparable

to the solenoidal field, the major to minor radii for the ATHENA e^+ ellipses will be approximately 25. Electrostatic effects would likely make this shape unstable. Even for more minor deformations, however, the elliptical profiles may reduce the overlap between the positrons and anti-protons, thereby reducing the \bar{H} production rate.

As with the mirror field, the most significant effect of the multipole field is likely to be increased transport. Experiments have demonstrated sharply increased transport with very small quadrupole fields; quadrupolar fields at the plasma edge 4000 times lower than solenoidal field have been shown to double the outward diffusion [9]. Preliminary data indicates that the diffusion increases linearly with quadrupole field strength when the quadrupole is strong [10]. To form a significant Minimum-B well, the quadrupole field would have to be comparable to the solenoidal field. Thus, the quadrupole might enhance diffusion by a factor of 4000.

The quadrupolar induced transport is strongest in the neighborhood of a resonance. Experimental data [9,11] suggests that the resonance occurs when the ratio nL/Bv_T remains constant, where n is the plasma density, L is the plasma length, B is the solenoidal field strength, and $v_T = \sqrt{kT/m}$ is the thermal velocity. This scaling is consistent with an orbital resonance; if a particle rotates by 90° during the time it takes to make one trap transit, then it can be on a trajectory that goes ever outwards or inwards [9]. While such resonant particles would be lost, there are too few precisely resonant particles to induce significant transport. However, there is a broad class of particles that are near resonance, which undergo large radial excursions. If these particles collide, their excursions will cause them to diffuse. The detailed theory of this Resonant Particle Transport is difficult to construct. Nonetheless, a back-of-the-envelope theory predicts transport of the right order of magnitude [11]. Disturbingly, the observed position of the resonance is off by a factor of two from the expected position. This discrepancy has lead Kabantsev and Driscoll to suggest [6] that the transport is more properly described by their Trapped Particle Scattering mechanism.

In the slowly rotating regime relevant here, the observed diffusion is inversely proportional to f_R^2 . If the ATHENA and ATRAP plasmas were off resonance by a factor of more than 50, the diffusion would be down to tolerable levels. Unfortunately, they are much closer than this to resonance (see Table 2) and the diffusion is likely to be very large.

5. Collisions

Both Trapped Particle Scattering Transport and Resonant Particle Transport occur only when the plasma particle orbits are disturbed by collisions [12–16]. Because plasma collision frequencies commonly increase with decreased temperature, and the plasmas considered here are very cold, the collision frequencies are typically large. There are three different, transport-inducing, collision categories: e^+e^+ collisions, $\bar{p}\bar{p}$ collisions, and $e^+\bar{p}$ collisions in the overlap region. Within each category, parallel–parallel, perpendicular–perpendicular, and parallel–perpendicular collisions may be described by different physics. Each type of collision will have a different collision frequency, and each will affect the transport in a different way. (Here parallel refers to motion along the magnetic field, and perpendicular to motion perpendicular to the field.)

The e^+e^+ collisions are complicated by the fact that the e^+ are in the strong magnetization regime; their cyclotron radius, $r_c = (c/eB)\sqrt{kT/m}$, is much less than their distance of closest approach, $b = e^2/kT$. In this regime, exchanges of perpendicular and parallel energy are strongly suppressed by O’Neil’s multiparticle collisional adiabatic invariant [13–15]. However, the frequency with which two e^+ exchange parallel velocities is not suppressed by the invariant. This frequency, $\nu_1 \approx nv_T b^2 \ln(\lambda_D/b)$, is very high: near 50 MHz for both ATHENA and ATRAP. The exchange of perpendicular energy between two e^+ is somewhat suppressed by the adiabatic invariant. The frequency for this type of exchange, $\nu_2 \approx nv_T b^2 (r_c/b)^2$, is near 20 kHz for ATHENA and 300 Hz for ATRAP. (The notation used here follows that in Ref. [13].)

In both experiments, the $\bar{p}\bar{p}$ collisions are in the transition region between the weakly and strongly magnetized regimes. Analytic expressions have not been found in this regime [15], but extrapolations suggest that the collision frequencies are near 100 Hz.

Lastly, collisions with the e^+ will affect the \bar{p} in the overlap region. If the two species were stationary with respect to each other, the collisions would be in the aforementioned transition region. However, the e^+ are drifting through the \bar{p} [1,2], which lessens the strong magnetization effects. The weak magnetization collision frequencies for drifting Maxwellians have been derived [17]. Unfortunately, the relative drift velocities for ATHENA and ATRAP are not available in the literature [1,2], so the collision frequencies cannot be evaluated precisely. Nonetheless the approximate frequencies can be found from $\nu_{\bar{p}e^+} \approx (nv_c b_c^2 m/M) \ln(\lambda_D/b_c)$, where m/M is the e^+ to \bar{p} mass ratio, and v_c and b_c are evaluated at some composite temperature incorporating both the relative drift and the two species’ intrinsic temperature. For plausible parameters, the collision frequencies will be in the neighborhood of 10 kHz. (Collisions with the \bar{p} will also affect the e^+ , but are unimportant because the \bar{p} density is much lower than the e^+ density.)

The collision frequencies given here are for $\sim 90^\circ$ collisions. With the exception of the parallel e^+e^+ collisions, the collisions result from sum of many small-angle collisions. As transport needs only small-angle collisions, the effective collision frequencies are substantially higher than the values given here. (The e^+e^+ collisions necessarily swap parallel velocities. Partial exchanges are forbidden [13]. However, parallel e^+e^+ collisions are already very frequent.)

The theories of Trapped Particle Scattering Transport and Resonant Particle Transport are not sufficiently developed to predict the dependence on the collision frequency, nor to determine the detailed consequences of the peculiarities of the strongly-magnetized collisions. It is unlikely that these peculiarities will have much effect on the velocity–space separatrix crossings integral to the Trapped Particle Scattering Transport. These peculiarities may have more effect on the

Resonant Particle Transport.² However, the transport may well wind up in the “plateau” regime [18] where the dependence on the collision frequency drops out.

In summary, particle collisions in ATHENA and ATRAP are frequent. A recent paper [19] contends that, because particles in Minimum-B fields orbit on unique, stable trajectories, transport will be insignificant. But the collisions described here disturb the orbits; proof of the stability of individual particle orbits is largely irrelevant to the issues of transport and loss.

6. High-order multipole advantages

As shown in Sections 3–5, quadrupole fields pose profound problems for e^+ and \bar{p} confinement. These problems may be alleviated by using higher-order multipole fields. The field from an infinitely-long multipole of order s scales with radius r as

$$|B| = B_{\max} \left(\frac{r}{R_w} \right)^{s-1} \quad (1)$$

where B_{\max} is the field at the wire radius R_w . For large order multipoles, the field is very small at the center. If a trap can be configured so that the e^+ and \bar{p} column radii are small compared to the wall radius, the constituents would be largely unaffected by the weak multipole field at the center. The resulting \vec{H} would still be trapped by the strong multipole field at the wall. For example, if the constituent radii were one-third of the wall radius, the multipole field magnitude were equal to the solenoidal field magnitude at the wall, and the multipole order was ten, the maximum field experienced by the constituents would be 20000 times less than the solenoidal field. Such multipole fields would be on the same order as the fields used in the quadrupole experiments [9], a level that is probably tolerable. Finite length effects and the

²Resonant particle transport theory requires collisions which change the parallel velocity. It is not clear whether the type of parallel velocity exchange permitted by O’Neil’s adiabatic invariant is sufficient. However, when combined with the parallel to perpendicular energy exchanges that result from inhomogeneities in the magnetic field magnitude, these collision should be sufficient to cause transport.

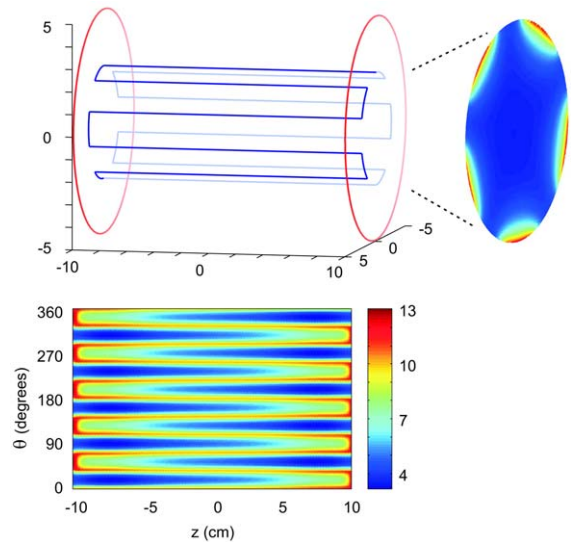


Fig. 4. Boundary magnetic field values for the configuration shown at top left. All magnetic field values are normalized to the field at the center. The multipole is fifth order with wires at radius 2.5 cm. The mirror coils are of radius 5 cm. The ratio of the current in the multipole to the current in the mirror coils is 1.45. In addition, there is an infinite solenoid, oriented along the configuration axis, which contributes 80% of the field in the center of the trap. The plot at the right shows the field at the end, and the bottom plot shows the “unwrapped” field along on the sides at 90° of the radius of the multipole wires, i.e. a cylinder of radius 2.25 cm. The minimum field occurs about 14% of the way in from the end on the side, and is of magnitude 3.16. The fields were calculated by numerical integration of Biot–Savart’s law in MATLAB.

addition of the mirror field complicate this picture somewhat, and the fields are best calculated numerically. The fields from a typical trial configuration are shown in Fig. 4.

One might worry that the greater degree of cancellation found in higher-order multipoles would require larger currents for the same field increase. An elementary calculation shows that this is not true. Assuming a sinusoidal current distribution, the required current density J_λ , in (A/m), is

$$J_\lambda = \frac{2B_{\max}}{\mu_0} \sin s\theta, \quad (2)$$

where B_{\max} is in Tesla. On gathering the current into $2s$ wires, the current in each wire drops

proportional to $1/s$, a favorable outcome. As an added benefit, the magnetic forces on each wire also decrease proportionally. Nonetheless, the currents, and hence the forces, are quite large; a tenth-order multipole that produces 1 T at wires arrayed at $R_w = 1$ cm requires currents on the order of 4000 A. It may be easier to create the required fields with permanent magnets; fortuitously, high-order multipole fields are easier to create with permanent magnets than are quadrupole fields.

Increasing the order of the multipole moves the multipole resonance to proportionally higher velocities. This can be favorable or unfavorable depending on the plasma parameters; it is likely to be favorable for ATHENA e^+ , but unfavorable for ATRAP e^+ .

A disadvantage of higher-order multipoles is that the \bar{H} trapping volume is relatively large; the multipole fields are not significant until the \bar{H} move far off the axis. This problem could be solved by turning on an auxiliary quadrupole to more tightly confine the \bar{H} once a sufficient number have been created and trapped in the high-order multipole.

7. Caveats

The loss of confinement predicted here is based on significant extrapolations from the current experimental data. The transport could saturate. The experiments and theory to date have studied mirror and quadrupole configurations separately. It is conceivable, but unlikely, that each will ameliorate the effects of the other. The model for the multipole transport is based on orbital resonances. The effects of the magnetron fields are difficult to calculate. Further, particularly for the \bar{p} , the rotation frequency is difficult to determine in the \bar{p} - e^+ overlap region. There may be very odd effects there. Finally, Kabantsev and Driscoll suggest that the proper mechanism for quadrupole induced transport is their Trapped Particle Scattering, not the Resonant Particle Diffusion mechanism presented here. However, the extrapolations are based on observational scalings, not theoretical predictions.

8. Conclusions

The tentative plans to trap \bar{H} in ATHENA and ATRAP need to be refined. The proposed mirror and quadrupole field are very likely to destroy the confinement of the \bar{H} constituents, e^+ and \bar{p} . Pushing the mirror field out beyond the constituent confinement region, and using a high-order multipole, may alleviate the \bar{H} constituent confinement problems. More exotic schemes are also available [20].

Acknowledgements

We thank Dima Budker, Gerry Gabrielse, Erik Gilson, Rolf Landua, Tom O'Neil, Ron Stowell and Gemma Testera for their helpful comments. This work was supported by the NSF.

References

- [1] M. Amoretti, et al., *Nature* 419 (2002) 456.
- [2] G. Gabrielse, N. Bowden, P. Oxley, A. Speck, C. Storry, J. Tan, M. Wessels, D. Grzonka, W. Oelert, G. Schepers, T. Seifick, J. Walz, H. Pittner, T. Haensch, E. Hessels, *Phys. Rev. Lett.* 89 (2002) 213401.
- [3] C.F. Driscoll, *Phys. Rev. Lett.* comment submitted; M.E. Glinsky, T.M. O'Neil Guiding center atoms: Three-body recombination in a strongly magnetized plasma, 3 (1991) 1279.
- [4] R. Gopalan, Studies of cryogenic electron plasmas in magnetic mirror fields, Ph.D. Thesis, University of California, Berkeley, 1998.
- [5] J. Fajans, *Phys. Plasmas* 10 (2003) 1209.
- [6] A. Kabantsev, C. Driscoll, *Phys. Rev. Lett.* 89 (2002) 245001.
- [7] A. Kabantsev, C. Driscoll, T. Hilsabeck, T. O'Neil, J. Yu, *Phys. Rev. Lett.* 87 (2001) 225002.
- [8] C.F. Driscoll, A.A. Kabantsev, T.J. Hilsabeck, T.M. O'Neil, Trapped-particle-mediated damping and transport, in: M. Schauer, T. Mitchell, R. Nebel (Eds.), *Workshop on Non-Neutral Plasmas 2003*, American Physics Society, New York, 2003, Vol. 692, p. 3.
- [9] E. Gilson, J. Fajans, *Phys. Rev. Lett.* 90 (2003) 01501.
- [10] E. Gilson, unpublished.
- [11] E. Gilson, Quadrupole induced resonant particle transport in a pure electron plasma, Ph.D. Thesis, University of California, Berkeley, 2001.
- [12] N. Rostoker, *Phys. Fluids* 3 (1960) 922.
- [13] T.M. O'Neil, *Phys. Fluids* 26 (1983) 2128.

- [14] B.R. Beck, J. Fajans, J.H. Malmberg, *Phys. Rev. Lett.* 68 (1992) 317.
- [15] M.E. Glinsky, T.M. O’Neil, M.N. Rosenbluth, K. Tsuruta, S. Ichimaru, *Phys. Fluids B* 4 (1992) 1156.
- [16] R. Stowell, R. Davidson, Kinetic theory of antihydrogen recombination schemes, in: M. Schauer, T. Mitchell, R. Nebel (Eds.), *Proceedings of the 2003 Non-Neutral Plasma Workshop*, American Physics Society, New York, 2003, Vol. 692, p. 162.
- [17] J. Huba, NRL plasma formulary, Technical Report NRL/PU/6790-02-450, Naval Research Laboratory, Washington, DC, 2002.
- [18] A. Galeev, R. Sagdeev, *Sov. Phys. JETP* 26 (1968) 233.
- [19] T. Squires, P. Yesley, G. Gabrielse, *Phys. Rev. Lett.* 86 (2001) 5266.
- [20] D.H.E. Dubin, *Phys. Plasmas* 8 (2001) 4331.
- [21] R. Landua, private communication.
- [22] G. Gabrielse, private communication.